Journal of Power Sources 195 (2010) 2731–2736

Contents lists available at ScienceDirect

Journal of Power Sources

journal homepage: www.elsevier.com/locate/jpowsour

Simulation of a supercapacitor/Li-ion battery hybrid for pulsed applications

D. Cericola, P.W. Ruch, R. Kötz*, P. Novák, A. Wokaun

General Energy Research Department, Paul Scherrer Institut, CH-5232 Villigen PSI, Switzerland

ARTICLE INFO

Article history:
Received 21 July 2009
Received in revised form
24 September 2009
Accepted 20 October 2009
Available online 2 December 2009

Keywords:
Battery
Capacitor
Supercapacitor
Ultracapacitor
Hybrid
Ragone plot

ABSTRACT

The direct parallel connection of a high energy Li-ion battery (MP 176065 Integration, Saft SA, France) and a supercapacitor (BCAP0310 P250, Maxwell Technologies Inc., Switzerland) was simulated using an available battery model in MATLAB/Simulink for various ratios of capacitor to battery energy content. The Ragone plots for the different combinations were calculated for constant power and pulsed power discharge, respectively. The Ragone plot of the hybrid device for constant power discharge shows an improved performance with respect to the capacitor in terms of available specific energy and an improved performance with respect to the battery in terms of available specific power. However, the combined device never meets the specific performance of the battery at high specific energy or of the supercapacitor at high specific power. For a pulsed discharge, however, the Ragone plots of the combined device show that the performance extends into an energy–power regime inaccessible to the single devices. The improved performance depends on the duty cycle of the pulse pattern and on the relative energy under each pulse.

1. Introduction

Batteries and supercapacitors (SCs) are electrochemical energy storage devices which utilize different mechanisms for the energy storage. While supercapacitors ideally store the electric energy in the electric field of the electrochemical double layer, batteries utilize the bulk of the respective electrode material for charge storage via redox reactions. As a consequence, the specific energy stored in an SC is relatively low due to limitations in the accessible specific surface area of the electrode, but the specific power is rather large due to the short time constant of double layer charging [1]. On the other hand, the specific energy of batteries is typically higher, but the specific power is relatively low due to almost unavoidable comparatively slow mass transport processes during charging and discharging. Therefore, a combination of both devices in a hybrid system appears to be reasonable. The idea to make use of the benefit of both devices – the high energy content of the battery and the high power of the SC – was realized by many research groups via the hybridization of the two devices within one system. The two main approaches for the hybridization of the two devices are (i) the combination of a battery electrode and a SC electrode within one cell [2–4] or (ii) the external hardwired parallel connection of batteries and SCs (external parallel hybrid, EPH). In electrical terms, however, the first approach represents a series connection of a battery and a capacitor, with the energy of the corresponding hybrid being limited by the capacitor and the power by the battery electrode. The EPH appears to be much more promising, because here the energy should be limited by the battery and the power by the capacitor. The performances of an EPH were assessed by different authors in different contexts. EPHs based on Li-ion batteries (LiBs) and SCs were studied by Chung et al. [5], Chandrasekaran et al. [6] and also by Sikha and Popov [7] in terms of Ragone plots. The properties of the hybrid device under pulsed load were investigated by Holland et al. [8], and the use of EPHs to suppress the fast transients in electric devices was investigated by Smith et al. [9]. These authors have shown the benefit of the hybridization in reducing the voltage drop and in extending the run time during pulsing. It has been emphasized that the specific energy of the hybrid is reduced with respect to that of the battery alone and that the size of the capacitor has to be tuned according to the characteristics of the pulse. The combination of a lead-acid battery with SCs for automotive applications was investigated by Bentley et al. [10] and Catherino et al. [11], again the advantage in delivering high power by the hybrid device in pulsed application was shown. A simple model to describe EPH was developed by Dougal et al. [12] and Sikha et al. [13] presented an "a priori" description of the parallel combination of a LiB and a commercial SC. An enhancement of the power performances and run time under pulsed application with respect to the battery was predicted from their calculations also in terms of Ragone plots.

A comparison of the different approaches is of course done best on the basis of the respective application. A somewhat more general comparison can be made on the basis of a so-called Ragone plot. Ragone plots are a long known and useful way to conveniently compare electrochemical energy storage devices on the basis of

* Corresponding author. Tel.: +41 56 310 2057; fax: +41 56 310 4415.
E-mail address: ruediger.koetz@psi.ch (R. Kötz).

0378-7753/$ – see front matter © 2009 Elsevier B.V. All rights reserved.
doi:10.1016/j.jpowsour.2009.10.104

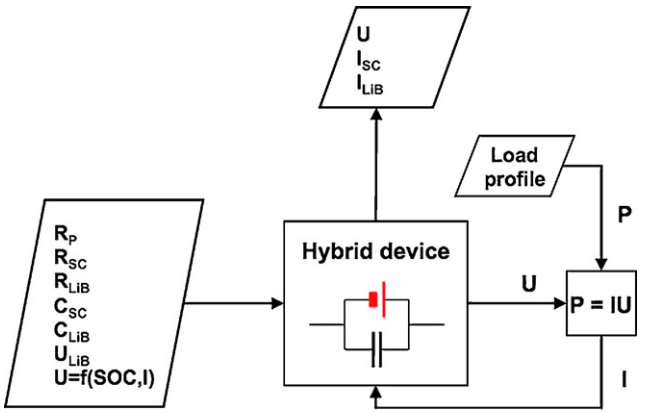

Fig. 1. Flowchart diagram representing the simulation routine.

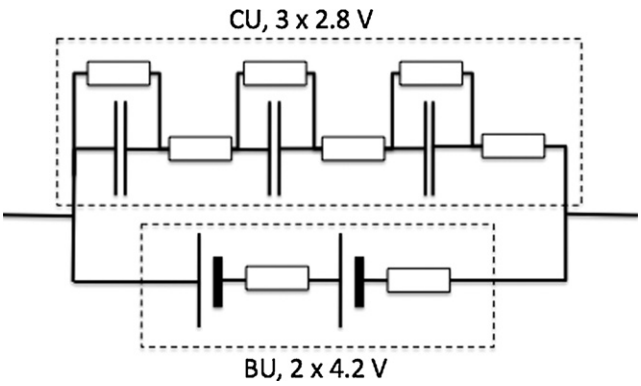

Fig. 2. Model of the hybrid device used in the calculations. A battery unit (BU) which consists of two batteries connected in series, is connected in parallel to a capacitor unit (CU) composed by the serial connection of three capacitors.

their energy–power relation [14]. Different Ragone plots can be constructed, the most frequent and original plot being that based on constant power discharge [14,15].

2. Simulation

MATLAB/Simulink (version 7.6.0.324) was used to simulate the parallel combination of a LiB with different numbers of SCs. The logic of the calculation is schematically represented by the flowchart in Fig. 1. The model of the hybrid device assumes the parallel connection of a battery and a capacitor without any interconnected electronics and without ohmic resistance of the connection. The battery behavior within the module is described by the model developed by Shepherd [16]. This model is a semi-empirical description of the discharge of a battery and does not take into account temperature and aging effects. The data needed for the model were taken from the data sheet of the high-energy LiB type MP 76065 Integration™ (Saft SA, France). This battery was selected as a state of the art high-energy battery with a specific energy of 180 Wh kg^{-1} according to the manufacturer.

For the simulation of the SC, a simple series RC connection with an additional leakage resistor parallel to the capacitor was assumed. Moss et al. [17] have demonstrated the applicability of this simple first-order description of the SC. The data for the internal equivalent series resistance (ESR) and the capacitance C_{SC} were taken from the data sheet for the BCAP0310 P250 (Maxwell Technologies Inc., Switzerland). The size of the leakage resistor R_P was calculated from the leakage current given in the data sheet after 72 h to be 5.5 kΩ at the nominal voltage of 2.5 V. The chosen SC is a power version of the Maxwell Technologies D-cell series.

In order to match the voltages of SC and LiB at full charge, a series connection of two batteries with a voltage window between U_{UP} = 8.4 V (2× 4.2 V) and U_{LOW} = 4.2 V was used. Throughout the paper this will be referred to as one battery unit (BU).

Parallel to the BU, three capacitors were placed in series, resulting in a maximum voltage for each capacitor of 2.8 V which is somewhat higher than the rated surge voltage of 2.7 V. The series combination of these three BCAP0310 P250 is defined as one capacitor unit (CU) throughout the paper. In this context, the capacitor configuration index (n) is defined as the number of CU connected in parallel to one BU (see Fig. 2).

A summary of the properties of the battery, capacitor, BU and CU is listed in Table 1.

As reported in Fig. 1, the hybrid device is simulated by the parallel connection of a battery model, which already includes the internal resistance of the LiB, and a conventional RC circuit representing the supercapacitor. The input for the calculation is made up of the ESR of the capacitor (R_{SC}), its capacitance (C_{SC}), and its parallel leakage resistance (R_P), the battery internal resistance (R_{LiB}), the charge capacity of the battery (C_{LiB}), and the battery voltage characteristic (U_{LiB}) which gives the voltage of the battery as a function of its state of charge and the charge and discharge current, respectively.

The current input (I) used in the hybrid model is evaluated in a feedback loop by dividing the desired power output (P) by the actual voltage output of the hybrid system (U) after correction for ohmic losses. Besides the voltage, further outputs of the simulation are the currents that flow in the BU (I_{LiB}) and in the CU (I_{SC}). The initial voltage of the hybrid device was set to 8.4 V. Each calculation was run with a defined power load pattern until the total charge available in the hybrid device was consumed. The load patterns used varied from a constant power discharge (hereafter called CP) to a pulsed discharge. The pulsed pattern is defined via two quantities: (i) the energy under each pulse (E_P) and (ii) the duty cycle (DC). The energy E_P is the amount of energy drawn during a single pulse. It is defined as a fraction of the total energy available in the hybrid system. The DC is defined as the ratio of the pulse duration to the time of one period. Therefore, a pulse pattern with a DC of 10%, an E_P of 0.4% and a period of 10 s consists of power pulses of 1 s followed by 9 s of rest, whereby the pulse amplitude discharges 0.4% of the total initial energy within one pulse. The E_P is inversely proportional to the number of pulses needed for complete discharge at

Table 1
Capacity, internal resistance, mass, specific energy and power for the battery, capacitor, BU and CU. The values for the single devices are stated in or estimated from the respective datasheets.

Element	Capacity/Ah	Internal resistance/mΩ	Leakage resistance/kΩ	Mass/g	Specific energy/Wh kg^{-1}	Specific power/kW kg^{-1}
Battery MP 176065 integration	6.8	33[a]		143	178	0.8[a]
Battery unit BU	6.8	66[a]		286	178	0.8[a]
Capacitor BCAP0310 P250	0.23 (at 2.7 V) (310 F)	2.2[b]	5.5[a]	60	4.48 (at 2.5 V)	23.6
Capacitor unit CU	0.24 (at 8.4 V) (103 F)	6.6[b]	16.5[a]	180	4.48 (at 7.5 V)	23.6

[a] Estimated from the data sheet.
[b] Direct current resistance.

low power, where the ohmic drop is considered negligible. A set of discharges under different power loads with the same defined load pattern enabled the construction of a complete Ragone plot. Different load patterns were used in order to investigate the effect of the load profile on the usable energy available in the hybrid system. In order to keep E_P constant, the pulse length has to be decreased when increasing the power and the pulse period has to be reduced to keep the respective DC. The energy of the system under investigation was evaluated by integration of the power with respect to time:

$$E = \int Px\,dt \tag{1}$$

where E is the energy, P is the power, and x is a function defined as:

$$x = \begin{cases} 1, & U_{LOW} \le U \le U_{UP} \\ 0, & \text{otherwise} \end{cases} \tag{2}$$

With U as the actual voltage of the hybrid device, U_{UP} as the initial voltage and U_{LOW} as the lower voltage cutoff.

The description of the capacitor used in the model does not include any frequency dependence of the capacitance and the ESR, which may underestimate the high power regime since the high frequency ESR drops to about half of the ESR at low frequency [18]. Moreover, the voltage dependence of the capacitance and ESR was neglected.

The Shepherd model [16] used to describe the discharge and charge of the battery assumes a constant internal resistance with respect to the state of charge. Charge capacity and internal resistance are also assumed to be independent of the discharge current. The model was developed with the oversimplified assumption that the sum of the overpotentials is linearly dependent on the current. It does not include any temperature effects. The model also neglects the contribution of the battery's double layer capacitance. A rough estimate, however, assuming an average specific surface area of 10 $m^2\,g^{-1}$ and a specific double layer capacitance of 10 $\mu F\,cm^{-2}$ for the composite electrode materials of the battery, shows that the battery capacitance will be in the order of 10 F, which is less than 5% of the capacitance of one BCAP0310 P250. Needless to stress, that under the assumptions made, the model is not suitable for describing the behavior of a high power battery in the high power region exactly.

3. Results and discussion

3.1. Constant power discharge

The Ragone plots for various combinations of one BU with CUs during constant power discharge are shown in Fig. 3 for $n = 1$, $n = 4$, and $n = 16$ together with the Ragone curves of the single units. From the model calculation the maximum specific energy of the battery is 178 Wh kg^{-1} and the maximum specific power is 800 W kg^{-1}, which is in good agreement with the data from the specification sheet. The capacitor has a maximum specific energy of about 4.2 Wh kg^{-1}, which is also in agreement with the datasheet specifications. The maximum specific power is 11 kW kg^{-1}, which is below the specified value due to the neglected frequency dependence of the ESR. In terms of maximum specific energy and power, all of the Ragone curves of the various hybrids fall below the curves of the single components.

From Fig. 3, it can be concluded that the specific performance of the hybrid device compared to the BU is improved by the combination with the CU ($n = 1$) in terms of increased power at very low energy; but at the expense of maximum energy and power at high energy. For the $n = 1$ combination, the maximum specific energy of the combination is reduced to 112 Wh kg^{-1} and the specific power

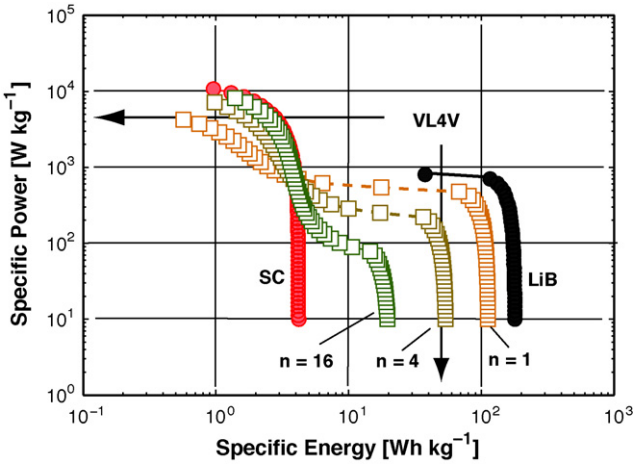

Fig. 3. Simulated Ragone plots for constant power discharge for the BU, CU (full symbols) and the $n = 1$, 4, and 16 combination (open symbols). As comparison the maximum specific energy and power of the very high power VL4V Saft battery are indicated by the arrows.

for specific energies below 2 Wh kg^{-1} is reduced to about 4 kW kg^{-1} compared to the maximum values of the respective single components.

On the other hand, the hybridization improves the specific performance of the hybrid device compared to the CU in terms of higher specific energy at low power, but at the expense of power at low energy. For $n = 16$, the maximum specific energy of the CU is increased up to 20 Wh kg^{-1} and the maximum specific power is reduced to 8 kW kg^{-1}. As a consequence, in the constant power regime, the combination of a battery with a capacitor does not exceed the performance of the single devices in the energy–power regime.

Also shown in Fig. 3 (arrows) is the maximum specific energy and maximum specific power for a state of the art very high power battery of comparable size (VL4V from Saft SA, France, 320g). With a maximum specific energy of 50 Wh kg^{-1} the energy is significantly lower than that of the high energy battery, but the maximum power for continuous discharge is stated by the manufacturer as 4.5 kW kg^{-1} for very high discharge currents [19]. With this battery as a benchmark, it is obvious that the combination of the capacitor and the high energy battery shows no improved performance compared to the single very high power battery for specific energies greater than 5 Wh kg^{-1}. This judgment, however, does not consider cost, efficiency, or lifetime considerations.

3.2. Pulsed power discharge

As opposed to the constant power discharge, a pulsed discharge pattern allows to obtain a specific performance with a combination of BU and CU which cannot be achieved with the single units. There are many applications where a pulsed power demand has to be satisfied, such as emergency generator start, start–stop cycles for micro- or mild hybrids and even GSM pulse patterns for mobile phones. Even the standard driving cycles defined for vehicle testing contain pulse patterns for urban driving in addition to almost steady state power on the highway. Naturally, the performance of the storage unit during pulsed discharge depends on the energy under each pulse and on the pulse frequency as described by the duty cycle.

The performance of an $n = 1$ combination of BU and CU is reproduced in Fig. 4a as a function of the energy under each pulse for a duty cycle of 10%. The energy under each pulse is given as a percentage of the total energy available. The power under each pulse was varied by variation of the current with simultaneous adapta-

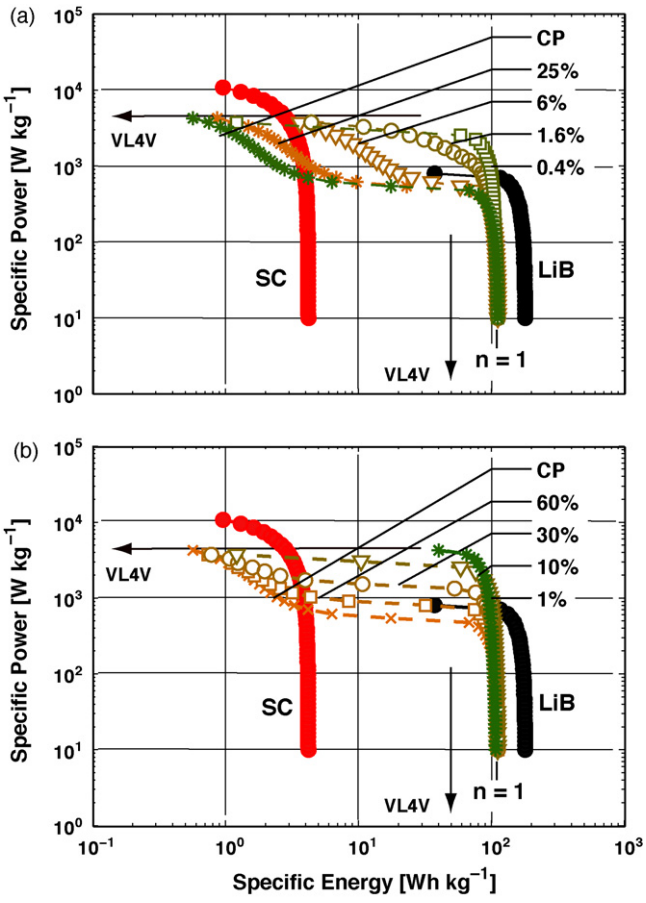

Fig. 4. Ragone plots for the $n = 1$ combination. (a) The energy under each pulse was varied, and the duty cycle was kept constant at 10%. (b) The energy under each pulse was kept constant at 0.4% of the maximum specific energy of the particular combination and the duty cycle was varied. The Ragone plots for the BU and CU at constant power discharge are shown for comparison (filled circles). The maximum specific energy and power for the very high power VL4V battery are indicated by the arrows.

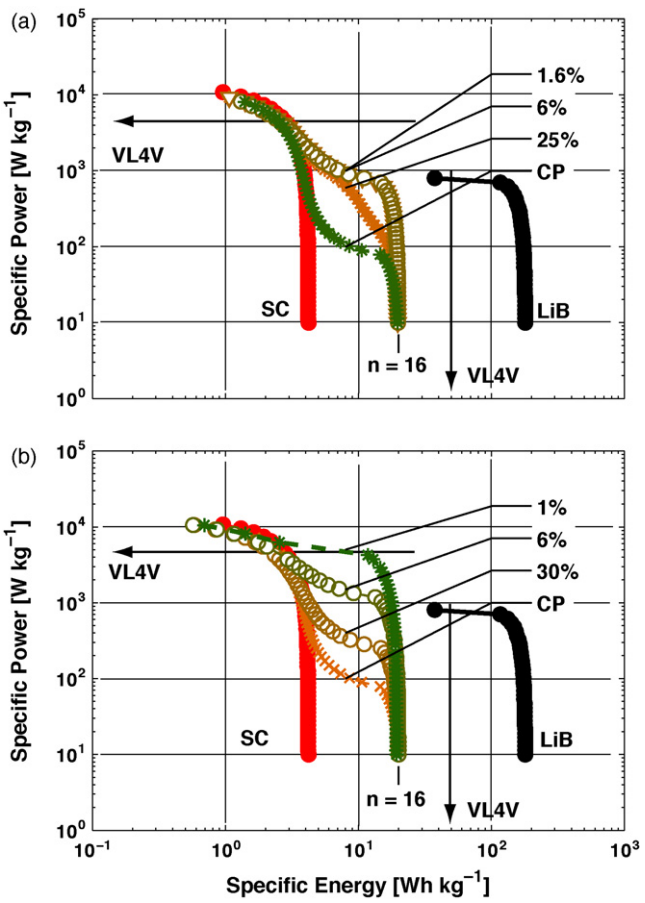

Fig. 5. Simulated Ragone plots for the $n = 16$ combination. Details are identical to Fig. 4.

tion of the pulse length and pulse period for constant E_P and DC. Therefore, the curve for 0.4% pulse energy describes a discharge of the storage device by about 250 pulses. Under these conditions, the maximum specific energy is reduced to 112 Wh kg^{-1} according to the increased mass of the $n = 1$ combination. However, the available power for each pulse is improved by about one order of magnitude compared to the battery unit alone. With increasing energy under each pulse, this improvement in specific power disappears and approaches the performance of the constant power discharge (see Fig. 3) for about 25% energy under each pulse (four pulses for total discharge).

The evolution of the specific performance (Ragone plot) of an $n = 1$ combination of CU and BU is shown in Fig. 4b as a function of duty cycle while keeping the energy under each pulse at the constant value of 0.4%. For a duty cycle of 1%, 10% and 30%, a clear increase in specific power is observed for high specific energy when compared to the BU alone. However, for a duty cycle of 60%, the performance decreases close to that obtained during constant power discharge. This is a very similar observation made experimentally and theoretically by Sikha et al. [13,7] (see Fig. 8 in [13] and Fig. 4 in [7]).

The combination of a large capacitor with a small battery is simulated in Fig. 5 for $n = 16$. Such a combination has a specific energy of about 20 Wh kg^{-1}, which is a significant improvement compared to the capacitor alone. Similar to the $n = 1$ combination, the power performance of the $n = 16$ combination is significantly increased when using a pulsed discharged compared to the CP discharge. As shown in Fig. 5a, a significant gain in performance is already available with pulses of 25% of energy, and there is no more gain when the energy under each pulse is reduced below 6%.

The effect of the duty cycle is reported in Fig. 5b. The Ragone plots were evaluated for $E_P = 0.4\%$ and exhibited a gain in power for reduced duty cycles. For a duty cycle of 1%, the Ragone plot corresponds to that of a SC with a specific energy of 20 Wh kg^{-1}.

The significant improvement in performance during pulse discharge over the performance during constant power discharge is simply due to the fact that the battery may recharge the capacitor between pulses. The share of power delivery during a pulse discharge with DC = 10% and $E_P = 0.4\%$ for a power of 2 kW kg^{-1} is shown in Fig. 6 for the $n = 1$ combination. During the pulse (of about 0.8 s) most of the power is supplied by the capacitor, while the battery recharges the capacitor during the rest period. The respective voltage decreases with the number of pulses, but a voltage recovering is observed during the recharging step in the rest period. It has to be emphasized that the specific power of the battery alone is limited to 0.8 kW kg^{-1}. In this example of pulsed discharge at 2 kW kg^{-1}, the average specific power provided by the battery during the complete pulsed discharge is 0.37 kW kg^{-1} with a maximum specific power of 0.44 kW kg^{-1}. These values are well below the applied specific power of 2 kW kg^{-1} and also well below the maximum specific power of the battery.

In the ideal case, the energy of the battery can be fully utilized at a power determined by the capacitor. In reality, however, the duty cycle, energy under each pulse, and power demand is given by the application. These dependencies are evaluated and represented in Fig. 7 for the $n = 1$ combination for specific power pulses of 1 and

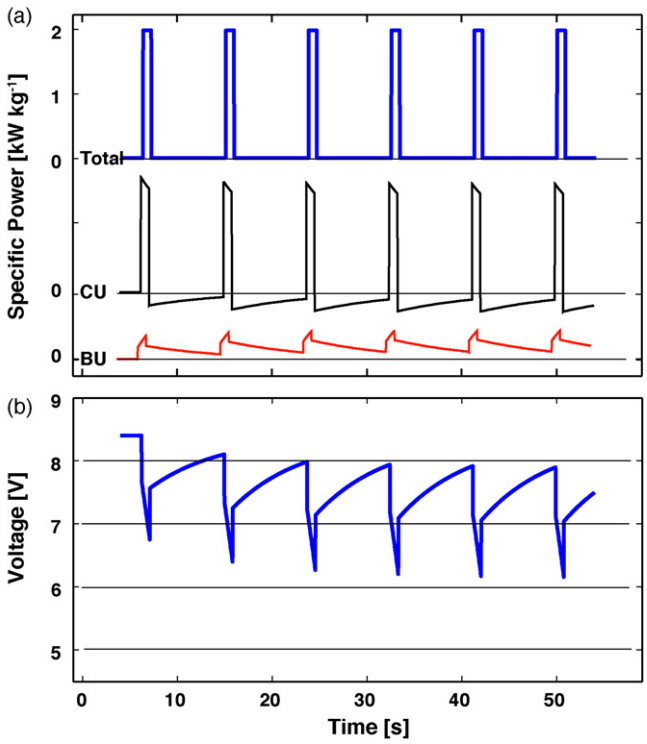

Fig. 6. (a) Power sharing between BU and CU and total power during pulsing at 2 kW kg^{-1} for the $n = 1$ combination. (b) Corresponding voltage profile of the hybrid device. The load pattern applied has an E_P of 0.4% and a DC of 10%. The power components have been calculated by multiplying the respective currents (I_{LiB} and I_{SC}) with the hybrid device voltage (U).

2 kW kg^{-1}. The specific energy available (in Wh kg^{-1}) under the different conditions is given by the color code. From Fig. 7, it is clear that a short duty cycle and short pulses (small energy per pulse) allow for the best utilization of the battery energy at a power not available for the battery alone.

Within a selected system, a long duty cycle (short rest period) limits the effectiveness of the recharging of the capacitor by the battery in the rest period. With a short duty cycle, this recharging

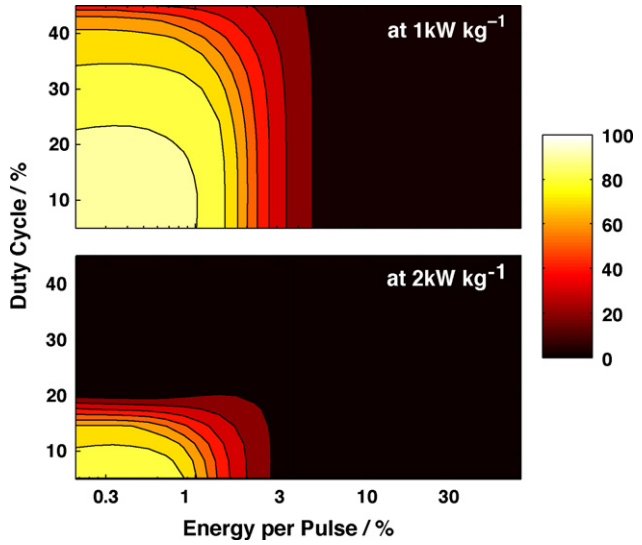

Fig. 7. Maps relating the energy available in the hybrid system as a function of the load pattern in terms of specific energy under each pulse and duty cycle for a specific power of 1 kW kg^{-1} (top) and 2 kW kg^{-1} (bottom). The available energy is defined by the color bar in Wh kg^{-1}.

is more complete and the available power at a certain energy is higher. Alternatively, the energy which can be taken during pulsed discharge for a given load profile is higher.

As it is shown in Fig. 6, the power and energy is mainly provided by the capacitor during the pulse. Therefore, the absolute energy under each pulse can be increased by increasing the number of capacitors in the CU.

Similarly, the $n = 16$ combination can provide reasonable power at an energy not available for the capacitor unit alone.

Depending on the load pattern, the hybrid system can provide similar or even better performance than the specifications of the very high power battery VL4V (Saft SA, France, Figs. 4 and 5).

It has to be considered that the above calculations do not include the use of any electronic energy management system for an optimized independent utilization of capacitor and battery energy flows. The performance of the hybrid devices considered can be certainly improved by the use of such an electronic system, but on the other hand such system will introduce additional mass and will also affect the reliability and cost.

Thus, the combination of readily available components within a supercapacitor–battery hybrid system is predicted to outmatch the state of the art very high power VL4V battery for certain load profiles. Further, it is expected that the lifetime of the hybrid device compares favorably with pure high power batteries due to the low power demand imposed on the battery. Other issues such as cycle life and cost are not discussed here, but need to be considered in the design of practically useful systems.

The application of our simple simulation approach to the power profiles of the various driving cycles for electric vehicles would be very interesting but would go beyond the scope of this paper. If, however, certain typical values for DC and E_P could be extracted from such driving cycles Fig. 7 could be used to estimate possible benefits of a battery–capacitor combination.

4. Conclusions

A systematic analysis of the performance of a hardwired parallel combination of state of the art rechargeable Li-ion battery and supercapacitor was presented. Because of the power sharing between the two devices, the specific energy and specific power of the hybrid system are extremely sensitive to the load pattern. Under constant power discharge, the performance of the investigated hybrid systems is intermediate to those of the battery and the capacitor alone, for which reason the hybridization does not provide an advantage over one of the single devices. However the available performance is significantly increased under pulsed load, and this was shown to be due to the recharging of the capacitor by the battery in the rest period between two subsequent pulses. As a general rule, shorter pulses and smaller duty cycles result in a higher available energy which can be taken from the hybrid system. Therefore, this approach allows to identify the optimal combination of capacitors and batteries according to the desired load pattern.

Acknowledgments

Swiss National Science Foundation is gratefully acknowledged for the financial support (Project no. 200021-117607). Very valuable and fruitful discussions with W. Scheifele (Paul Scherrer Institut) are gladly appreciated.

References

[1] R. Kötz, M. Carlen, Electrochimica Acta 45 (2000) 2483–2498.
[2] V. Khomenko, E. Raymundo-Pinero, F. Beguin, Journal of Power Sources 177 (2008) 643–651.
[3] G.G. Amatucci, F. Badway, A. Du Pasquier, T. Zheng, Journal of the Electrochemical Society 148 (2001) A930–A939.

[4] M.S. Hong, S.H. Lee, S.W. Kim, Electrochemical and Solid-State Letters 5 (2002) A227–A230.
[5] K.I. Chung, J.S. Lee, Y.O. Ko, Journal of Power Sources 140 (2005) 376–380.
[6] R. Chandrasekaran, G. Sikha, B.N. Popov, Journal of Applied Electrochemistry 35 (2005) 1005–1013.
[7] G. Sikha, B.N. Popov, Journal of Power Sources 134 (2004) 130–138.
[8] C.E. Holland, J.W. Weidner, R.A. Dougal, R.E. White, Journal of Power Sources 109 (2002) 32–37.
[9] T.A. Smith, J.P. Mars, G.A. Turner, IEEE 33rd Annual Power Electronics Specialists Conference, vol. 1, 2002, pp. 124–128.
[10] P. Bentley, D.A. Stone, N. Schofield, Journal of Power Sources 147 (2005) 288–294.
[11] H.A. Catherino, J.F. Burgel, P.L. Shi, A. Rusek, X.L. Zou, Journal of Power Sources 162 (2006) 965–970.
[12] R.A. Dougal, S. Liu, R.E. White, IEEE Transactions on Components and Packaging Technologies 25 (2002) 120–131.
[13] G. Sikha, R.E. White, B.N. Popov, Journal of The Electrochemical Society 152 (2005) A1682–A1693.
[14] D.V. Ragone, Review of Battery Systems for Electrically Powered Vehicles, Mid-Year Meeting of the Society of Automotive Engineers, Detroit, MI, May, 1968, pp. 20–24.
[15] T. Christen, M.W. Carlen, Journal of Power Sources 91 (2000) 210–216.
[16] C.M. Shepherd, Journal of The Electrochemical Society 112 (1965) 657–664.
[17] P.L. Moss, J.P. Zheng, G. Au, P.J. Cygan, E.J. Plichta, Journal of The Electrochemical Society. 154 (2007) A1020–A1025.
[18] R. Kötz, M. Hahn, R. Gallay, Journal of Power Sources 154 (2006) 550–555.
[19] http://www.saftbatteries.com/doc/Documents/defence/Cube770/Systems%2Brochure_final.f44756e4-2c47-4fb8-9e72-8a6fdc0d7410.pdf (last visited on 15.07.2009).